Bank Erosion by Wind-Generated Waves: Development of the Wind-Wave Sub-Model in BSTEM-Dynamic

Yavuz Ozeren, Research Assistant Professor, National Center for Computational Hydroscience and Engineering, University of Mississippi, University, MS, yozeren@ncche.olemiss.edu
Andrew Simon, Technical Director Senior Principal - Geomorphology/Modeling, Stantec, Oxford, MS, Andrew.Simon@cardno.com
Jennifer Hammond, Senior Project Engineer
Cardno Newark, DE, Jennifer.Hammon@cardno.com

Abstract

To estimate the relative contribution of wind-generated waves on streambank erosion and provide reliable tools for the analysis of bank-retreat processes and effective mitigation strategies, a wind-generated wave erosion module was developed and incorporated to the BSTEM-Dynamic code (v. 2.4). Additional bed shear stress resulting from wind-generated waves was calculated by considering wave transformation and breaking along the bank profile. The estimated significant wave height (H_{mo}) and peak wave period (T_p), were compared with field measurements of wind and waves at two sites located along a 29-km reach of Tennessee River between Pickwick Dam and Savannah, TN where the new model was tested for the period between 1985 and 2016 using the wind data from Muscle Sholes Airport, AL. This paper presents the theoretical background for the wind-wave prediction method and shear-stress estimation procedures.

Introduction

In general, wind-generated waves are not an important concern in rivers due to the limited fetch length and flow depth. However, wind-generated waves can become large enough to have a significant impact on the banks of large, wide, impounded rivers, large canals and embayments. A considerable amount of bank erosion was attributed to boat and wind-generated waves along some reaches of the Illinois River (Bhowmik and Schicht, 1980). Significant wave heights of 0.4 m were calculated for 2-year return period winds of 6-hr duration on the Mississippi River (Bhowmik et al., 1982). Excessive turbidity in the near-bank zone, indicative of localized bank erosion was observed along some reaches of Connecticut and Tennessee River by the authors.

Combined with the streamflow, recurrent wave action can lead to undercutting and eventual failure of the upper part of the bank. Estimation of the relative contribution of wind-generated waves to streambank erosion requires the prediction of the wave properties on the bank-line for varying wind conditions and their impact on the streambank. In this study, a wind-generated wave-erosion module was developed and incorporated to the BSTEM-Dynamic code (v. 2.4) with the goal of providing reliable tools for the analysis of bank-retreat processes and effective mitigation strategies. The underlying assumption for the development of this module is that the waves contribute to streambank erosion with the additional boundary shear stress due to the orbital motion of the waves above the bank surface. With the provided wind speed and direction,

the module calculates the sizes of the generated waves and applies an additional shear stress along the bank surface by considering wave transformation in the surf zone.

Model Development

BSTEM-Dynamic (v. 2.4) uses geotechnical-stability and hydraulic-erosion algorithms for deterministic analysis of bank stability over varying flow stages. The geotechnical-stability module determines the potential failure plane automatically by an iterative search routine that locates the most critical failure-plane. The hydraulic-erosion algorithm uses the excess shear-stress approach to calculate the erosion rate on the back face. The model updates the bank geometry at each time step based on the calculated hydraulic erosion and any critical failure planes. In this way, the model can predict streambank retreat for a time series of flows decades in length. BSTEM-Dynamic has been applied in diverse environments in the United States and across the globe.

Wind-Wave Generation

Wind waves originate as a result of the water-surface disturbances due to the pressure fluctuations within the wind field. The shear stress between the air and water interface that is exerted by wind is the driving force for the waves. It is commonly estimated using local wind-field measurements at a specific location and height. The waves keep growing in height and length with increasing wind speed, wind duration and the distance over which the wind blows (fetch length). If the wind duration exceeds the time required for waves to propagate the entire fetch length, the characteristics of the generated waves, namely the significant wave height (H_{mo}) and peak wave period (T_p), as well as the resulting spectrum of wind-generated waves depend primarily on the fetch length and wind speed. These conditions are typically met in restricted waters. At relatively shallow water depths, bottom friction also becomes important and can be a limiting factor for wave growth. To calculate the wind-generated wave properties (H_{mo} and T_p) for a given set of wind speeds and fetch lengths (U and F), the Joint North Sea Wave Project (JONSWAP) wave-prediction method was incorporated into BSTEM-Dynamic. JONSWAP wave growth prediction method is described as (Hasselmann et al., 1973):

$$\frac{gH_{m0}}{U^2} = 0.0016\left(\frac{gF}{U^2}\right)^{1/2} \tag{1a}$$

$$\frac{gT_p}{U} = 0.286\left(\frac{gF}{U^2}\right)^{1/3} \tag{1b}$$

$$\frac{gt_{min}}{U} = 68.8\left(\frac{gF}{U^2}\right)^{2/3} \tag{1c}$$

where, g is gravity, and the time t_{min} is the minimum duration for the waves to become fetch-limited assuming deepwater group wave speed, $c_g = \frac{gT_p}{4\pi}$ is valid. Here, U refers to the direct measurement of wind speed at 10 m height over the water surface.

Wave growth is limited with fully developed conditions which are defined by:

$$\frac{gH_{m0}}{U^2} = 0.243 \quad \text{and} \quad \frac{gT_p}{U} = 8.134 \tag{2}$$

Wave Transformation

Waves approaching the shoreline transform by the changes in the bottom contours. As the waves propagate from deep to shallow water, their height, length and speed change. Also, waves obliquely approaching shallow water assume a direction normal to the depth contours due to the slower wave-propagation speed in shallow water. These transformations are considered in the BSTEM-Dynamic wind-wave module.

Wave height was adjusted to account for shoaling (change in wave height) and refraction (change in direction) using the equations below:

$$H = K_s K_r H_0 \tag{3}$$

where,

$$K_s = \sqrt{\frac{n_1}{n_2}\frac{L_1}{L_2}} \quad \text{and} \quad K_r = \sqrt{\frac{\cos\theta_1}{\cos\theta_2}}. \tag{4}$$

Here, L is the wave length, $n = \frac{1}{2}\left(1 + \frac{2kh}{\sinh 2kh}\right)$, and the wave number, $k = \frac{2\pi}{L}$. The subscripts 1 and 2 indicate successive wave crests. The angle θ is calculated Snell's law, namely $c_1/\sin\theta_1 = c_2/\sin\theta_2$ in which c_1 and c_2 are wave celerity at two consecutive wave crests.

The breaking criterion for a horizontal bed is given by (Miche, 1944):

$$\frac{H_b}{L_b} = \frac{1}{7}\tanh(k_b h_b) \tag{5}$$

The limiting wave height is approximated using a solitary wave in shallow water (McCowan, 1894; Munk, 1949):

$$\frac{H_b}{h_b} = 0.78 \tag{6}$$

The runup height, R is estimated in terms of beach slope using empirical formulae:

$$R = \tan\beta\sqrt{H_0 L_0} \text{ for } 0.1 < \xi_0 < 2.3 \text{ (Hunt 1959)} \tag{7a}$$

$$R = 1.38\,\xi_0^{0.7} \text{ for } 2.3 < \xi_0 \text{ Mase (1989)} \tag{7b}$$

where, the surf similarity parameter is, $\xi_0 = \tan\beta\,(H_0/L_0)$.

Wave erosion and sediment transport

In shallow water, the orbital velocities of the waves near the bed create an additional shear force on the bed material. Wave related bed shear stress depends on the horizontal orbital velocity and the friction factor. The maximum horizontal velocity near the bed is calculated based on linear wave theory as:

$$U_w = \sigma A_w \tag{8}$$

where, the wave angular frequency, $\sigma = T/2\pi$, and the peak excursion, $A_w = H_m/2\sinh(kh)$. The bed shear stress is:

$$\tau_w = \frac{1}{2}\rho f_w U_w^2 \tag{9}$$

The bed shear stress oscillates and changes direction with the waves but the friction factor f_w is assumed to be constant over the wave cycle (Van Rijn, 1993). Definition of the friction factor varies based on the flow conditions which can be characterized by the wave related Reynolds number, $\mathrm{Re}_w = U_w h/\nu$. Hydrodynamically smooth and rough conditions are defined as follows (Jonsson, 1966, 1980):

$f_{ws} = 0.9\mathrm{Re}_w^{-0.2}$ smooth, turbulent flows (Van Rijn, 1993) $10^4 < \mathrm{Re}_w < 10^6$ and $A_w/k_s > 10^3$

$f_{wr} = \exp\left[-6 + 5.2\left(\frac{A_w}{k_s}\right)^{-0.19}\right]$ rough, turbulent flows (Swart, 1976) $10^5 < \mathrm{Re}_w$ and $A_w/k_s < 100$

where k_s is the roughness height and can be approximately calculated using median grain diameter (Madsen et al., 1993):

$$k_s = 15 d_{50} \tag{10}$$

In the existence of both current and waves, the total instantaneous bed shear stress, $\boldsymbol{\tau_T}(t)$ has two components: the oscillating wave-related bed shear stress, $\boldsymbol{\tau_w}(t)$, and the non-oscillating current-related bed shear stress, $\boldsymbol{\tau_0}$. Hence, the total shear stress is also time dependent and oscillates in a wave cycle. Neglecting the nonlinearities due to turbulence (Soulsby and Clarke, 2005), at any time (t), the total bed shear stress is given by the vector sum of the two:

$$\boldsymbol{\tau_T}(t) = \boldsymbol{\tau_0} + \boldsymbol{\tau_w}(t) \tag{11}$$

Using sinusoidal assumption and the magnitudes of the shear-stress vectors, root-mean-square shear stress is calculated by:

$$\tau_{rms} = \sqrt{\tau_0^2 + \frac{1}{2}\tau_w^2} \tag{12}$$

BSTEM implementation

When the wind-wave module is activated, BSTEM-Dynamic (v.2.4) reads the wave data in the "wind-generated wave output" section of the "Wind Wave" tab for wave-erosion calculations (Figure 1). If the user provides the wind speed, direction and fetch length, the module estimates the wave properties at a given location using JONSWAP method. The "shore normal angle" is the direction of the shoreline normal relative to north, and it is required when wind-wave prediction is requested. If the angle between wind direction and the shore normal is greater than 80 degrees, wind waves are not included in the calculations.

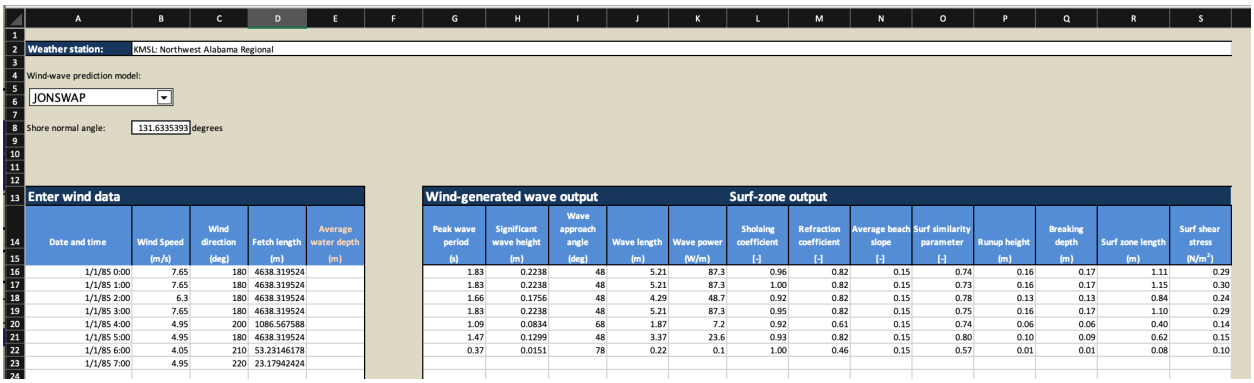

Weather station: KMSL: Northwest Alabama Regional

Wind-wave prediction model: JONSWAP

Shore normal angle: 131.6335393 degrees

Enter wind data

Date and time	Wind Speed (m/s)	Wind direction (deg)	Fetch length (m)	Average water depth (m)
1/1/85 0:00	7.65	180	4638.319524	
1/1/85 1:00	7.65	180	4638.319524	
1/1/85 2:00	6.3	180	4638.319524	
1/1/85 3:00	7.65	180	4638.319524	
1/1/85 4:00	4.95	200	1086.567588	
1/1/85 5:00	4.95	180	4638.319524	
1/1/85 6:00	4.05	210	53.23146178	
1/1/85 7:00	4.95	220	23.17942424	

Wind-generated wave output | **Surf-zone output**

Peak wave period (s)	Significant wave height (m)	Wave approach angle (deg)	Wave length (m)	Wave power (W/m)	Sholaing coefficient [-]	Refraction coefficient [-]	Average beach slope [-]	Surf similarity parameter [-]	Runup height (m)	Breaking depth (m)	Surf zone length (m)	Surf shear stress (N/m^2)
1.83	0.2238	48	5.21	87.3	0.96	0.82	0.15	0.74	0.16	0.17	1.11	0.29
1.83	0.2238	48	5.21	87.3	1.00	0.82	0.15	0.73	0.16	0.17	1.15	0.30
1.66	0.1756	48	4.29	48.7	0.92	0.82	0.15	0.78	0.13	0.13	0.84	0.24
1.83	0.2238	48	5.21	87.3	0.95	0.82	0.15	0.75	0.16	0.17	1.10	0.29
1.09	0.0834	68	1.87	7.2	0.92	0.61	0.15	0.74	0.06	0.06	0.40	0.14
1.47	0.1299	48	3.37	23.6	0.93	0.82	0.15	0.80	0.10	0.09	0.62	0.15
0.37	0.0151	78	0.22	0.1	1.00	0.46	0.15	0.57	0.01	0.01	0.08	0.10

Figure 1. A screenshot of the "Wind Wave" tab in BSTEM-Dynamic (v.2.4)

Surf-zone output parameters such as average shoaling and refraction coefficients, surf similarity parameter, and runup height are calculated using the average bank slope, which is defined as the slope of the straight line from the last dry bank point to the point riverward of the breaking point. Adverse (negative) slope is allowed, but inverse (avearge slope $> \pi/2$) is set to vertical. The slope of the swash zone, defined as the slope of the bank segment between the last dry bank point and its offshore neighbor, is used to calculate runup distance and the last dry bank point is adjusted based on the runup along this slope.

Field Measurements

Estimated values of H_{mo} and T_p, were compared with field measurements at two sites located along a reach of Tennessee River between Pickwick Dam and Savannah, TN (Figure 2a and 2b). At each site, waves were measured by 3 m-long capacitance type wave staffs with a 30 Hz measurement frequency. Wind speed and direction were measured using a HOBO RXW Davis Wind Speed & Direction Sensor. The fetch was obtained by measuring the straight-line distance along the wind direction from the site to the bankline. The fetch lengths measured by this method at site 1 are shown in Figure 2c. The sensor was set to record wind speed at 1-minute intervals. Then, 15-minute average wind speed and direction were down-sampled for wind-wave prediction analysis.

The wind rose in Figure 2d shows the wind speed and direction measured at site 1 for the period between 6/19/2020 - 8/3/2020. The highest winds for the measurement period were form southeast. Comparison with the Muscle Shoals, AL Northwest Alabama Regional Airport station (approximately 43 miles away) indicated that the measured wind data at site 1 was apparently filtered out by the trees and the riverbank in the southeast and northwest directions.

Wind speed exceeded 20 mph (~10 m/s) for some storm events during the measurement period. These winds generated significant wave heights as high as 15 cm at site 1 and 25 cm at site 2. Figure 3 shows an example of wind speed and direction data compared with wave height and period at site 2 for the period between August 27 - 29, 2020. River stage and the calculated fetch length are also shown in the same figure. To test the JONSWAP method with the measured data, two intervals were selected in the recoded time period, during which the wind speed was significantly high, wind direction was in line with the longest fetch and boating activity was minimum. Figure 4 compares the measured data at sites 1 and 2 with JONSWAP predictions. The agreement between the measured data and JONSWAP prediction was considered reasonably good.

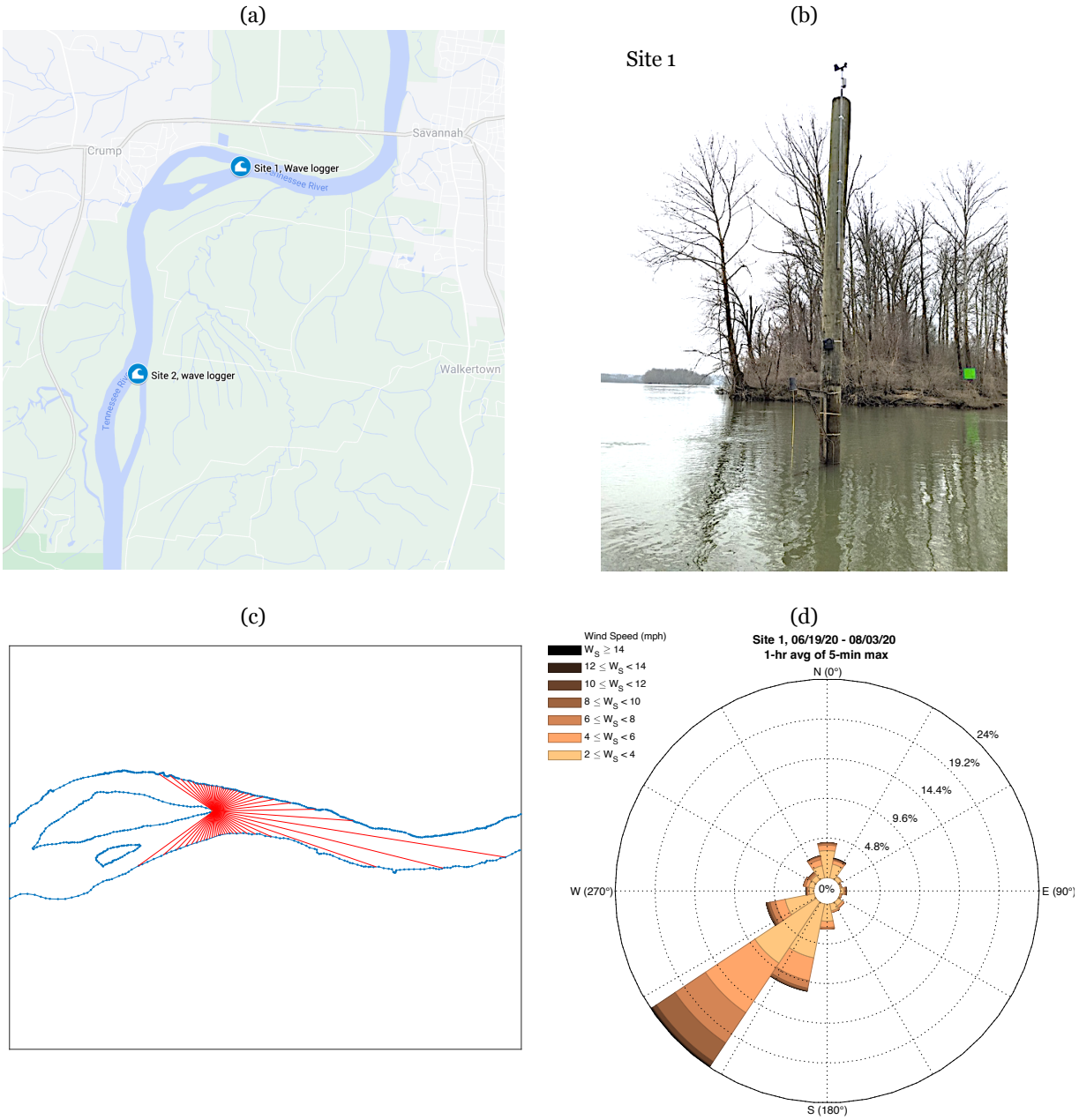

Figure 2. (a) Wind and wave monitoring sites; (b) the wave logger and wind gauge at site 1; (c) fetch lengths for the possible directions over the water; (d) wind rose at site 1 for the measurements between 6/19/20 - 8/30/20

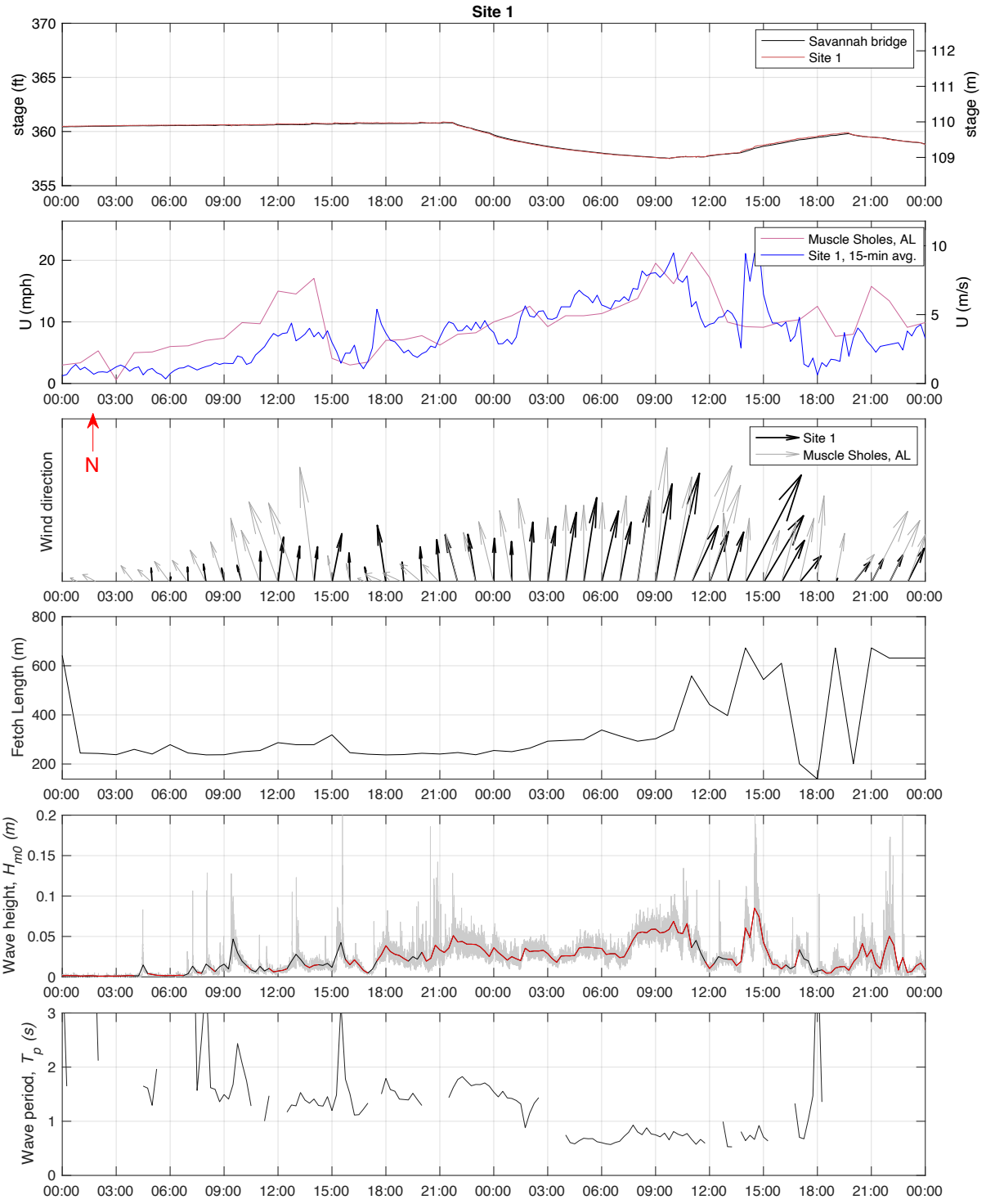

Figure 3. Stage, wind speed and direction, fetch length, and wave height and period comparison at site 1 between August 27 - 29, 2020

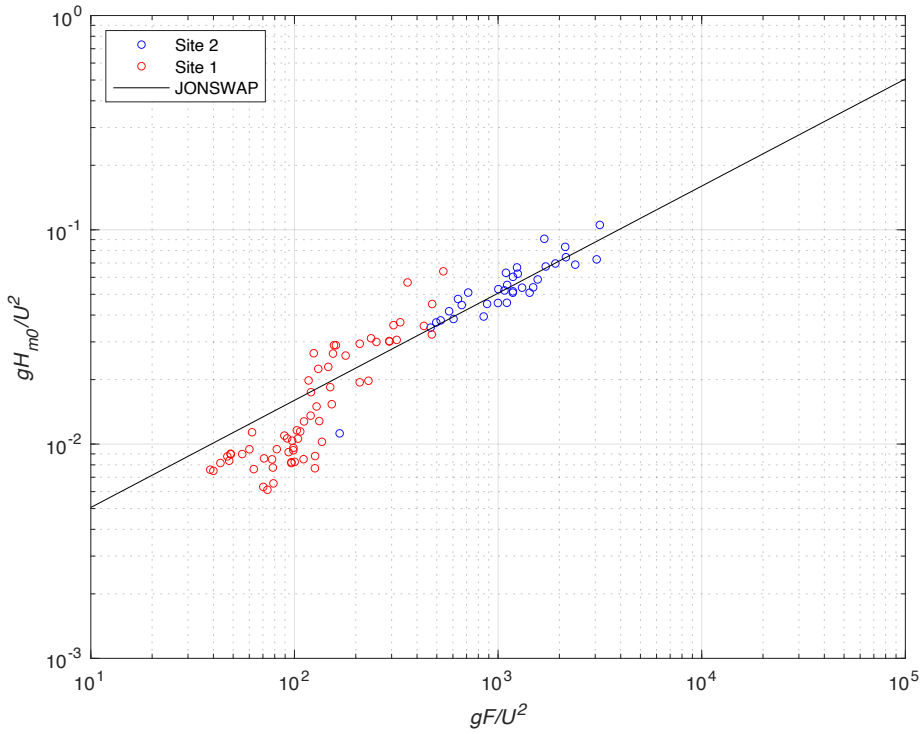

Figure 4. Dimensionless wind and wave parameters compared with JONSWAP wind prediction

Conclusions

A new sheet was added to BSTEM-Dynamic (v. 2.4) that includes modules that were developed to estimate wind-wave properties, significant wave height (H_{mo}) and peak-wave period (T_p) using the provided wind speed and fetch length. Additional bed shear stress resulting from wind-generated waves was calculated by considering wave transformation and breaking along the bank profile. The predicted wave height and period compared reasonably well with the measured values for some storm events during the field campaign. The updated BSTEM-Dynamic model was applied to two studies with the objective of evaluating the relative roles of various bank-erosion processes on rates of erosion and bank retreat. The findings of these studies, which are discussed in more detail in the following companion paper (Simon et al., this volume), showed that BSTEM-Dynamic can be an effective tool for evaluating the relative contribution of waves on streambank erosion.

References

Bhowmik, N.G., Demissie, M., Guo, C.Y., 1982. “Waves Generated by River Traffic and Wind on the Illinois and Mississippi Rivers,” WRC Research Report, No. 167. University of Illinois, Urbana.

Bhowmik, N.G., Schicht, R.J., 1980. “Bank Erosion of the Illinois River,” Report of Investigation, No. 92. Illinois Institute of Natural Resources, Urbana.

Hasselmann, K., Barnett, T.P., Bouws, E., Carlson, H., Cartwright, D.E., Enke, K., Ewing, J.A., Gienapp, H., Hasselmann, D.E., Kruseman, P., Meerburg, A., Müller, P., Olbers, D.J., Richter,

K., Sell, W., Walden, H., 1973. “Measurements of wind-wave growth and swell decay during the joint north sea wave project (JONSWAP)”.,Dtsch. Hydrogr. Z. Suppl. 8A (12), 95.

Hunt, I.A., 1959. “Design of seawalls and breakwaters,” Journal of the Waterways and Harbors Division, 85, 123–152.

Jonsson, I., 1966. Wave boundary layers and friction factors. In: Proc. 10th Int. Conf. Coastal Eng. ASCE, Tokyo, Japan, pp. 127–148.

Jonsson, I., 1980. A new approach to oscillatory rough turbulent boundary layers. Ocean Engineering 7, 109–152.

Madsen, O. S., Wright, L. D., Boon, J. D., & Chisholm, T. A. (1993). Wind stress, bed roughness and sediment suspension on the inner shelf during an extreme storm event. *Continental Shelf Research*, *13*(11), 1303-1324.

Mase, H., 1989. “Random wave run-up height on gentle slopes,” Journal of Waterway, Port, Coastal, and Ocean Engineering, 115, 649-661.

McCowan, J., 1894. “On the highest wave of permanent type,” The London, Edinburgh, and Dublin Philosophical Magazine and Journal of Science, *38*(233), pp.351-358.

Miche, M., 1944. Le pouvoir reflechissant des ouvrages maritimes exposes a l'action de la houle. Ann. Ponts Chaussees. 121, 285–318.

Munk, H.W., 1949. “Solitary Wave and Its Application to Surf Problems,” Annals, New York Academy of Science, Vol. 51, pp. 376–424.

Swart, D. 1976. “Predictive equations regarding coastal transports”, Coastal Engineering Proceedings, 1(15), 65.

van Rijn, L.C., 1993. Principles of sediment transport in rivers, estuaries and coastal seas. Aqua Publications, Amsterdam, The Netherlands.